Supplementary Information for Journal of Analytical Methods

# A novel low-rank coal-based CDs for the detection of $Fe^{3+}$

Wenwen Wu, Xiang Han*, Siyu Zhang, Lele Li, Meili Du, Fuxin Chen
College of Chemistry and Chemical Engineering，Xi’an University of Science and Technology，Xi’an 710054,China

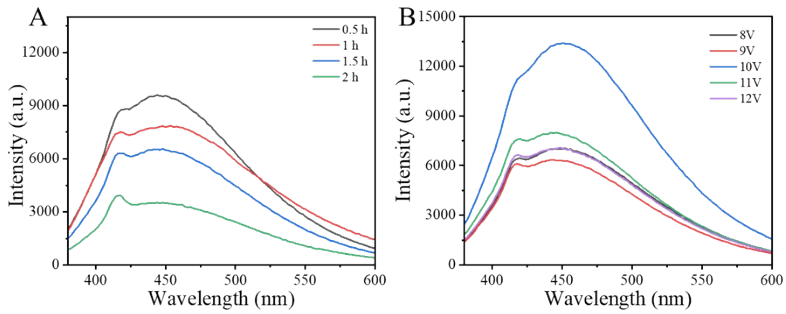


**Fig. S1: A: Fluorescence spectra of coal-based CDs prepared at different reaction times；B：Fluorescence spectra of coal-based carbon dots prepared at different voltages.**

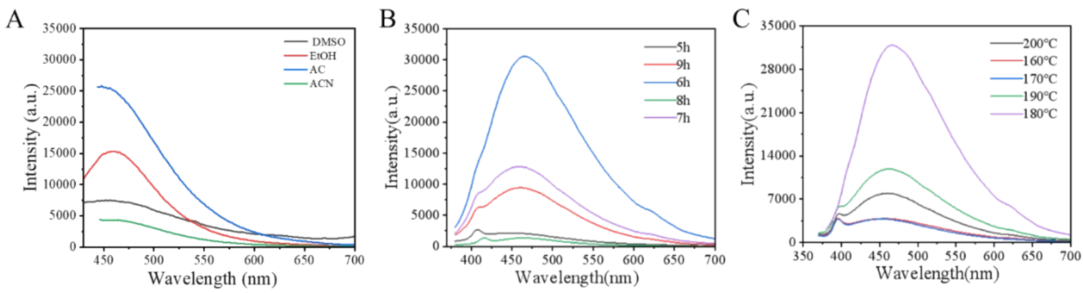


**Fig. S2：A: Coal-based CDs prepared by DMSO, EtOH, AC, ACN；B: Coal-based CDs prepared at different times C: Fluorescence spectra of coal-based CDs prepared at different temperatures.**

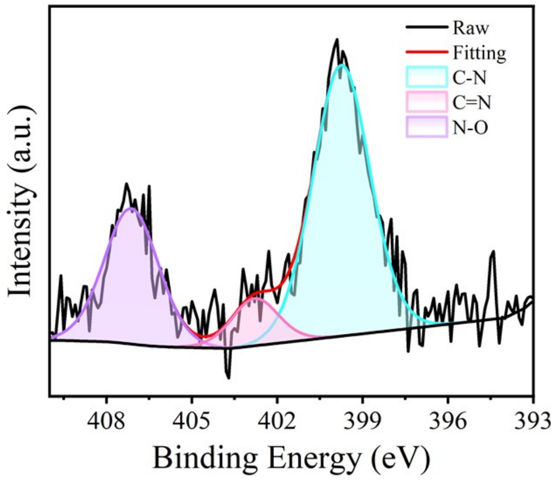


**Fig. S3 The high-resolution N1s spectrum of CDs XPS.**

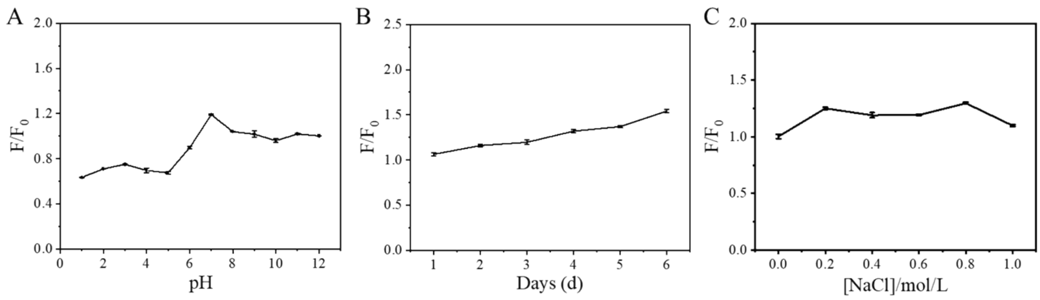


**Fig. S4: A: The influence of pH on the fluorescence intensity of coal-based CDs; B: The influence of time on the fluorescence intensity of coal-based CDs; C: The influence of ion concentration on the fluorescence intensity of coal-based CDs.**

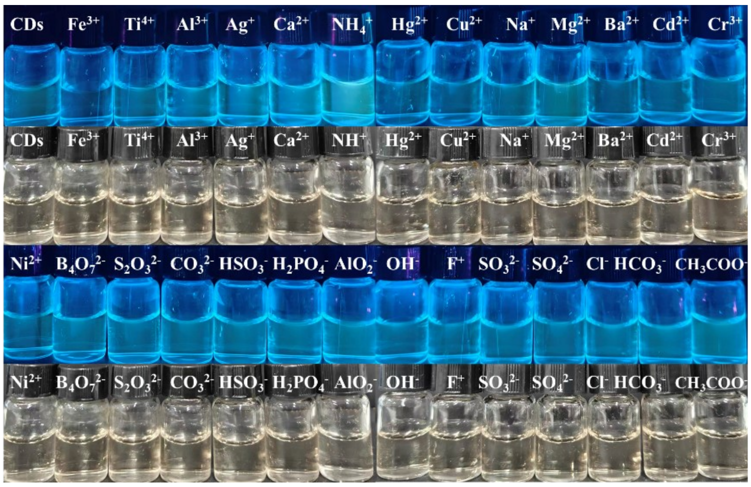

**Fig. S5 Changes in color and fluorescence of CDs solution (100μM) upon addition of different ions (CDs, $Fe^{3+}$, $Ti^{4+}$, $Al^{3+}$, $Ag^{+}$, $Ca^{2+}$, $NH_4^{+}$, $Hg^{2+}$, $Cu^{2+}$, $Na^{+}$, $Mg^{2+}$, $Ba^{2+}$, $Cd^{2+}$, $Cr^{3+}$, $Ni^{2+}$, $B_4O_7^{2-}$, $S_2O_3^{2-}$, $CO_3^{2-}$, $HSO_3^{-}$、$H_2PO_4^{-}$, $AlO_2^{-}$, $OH^{-}$, $F^{-}$, $SO_3^{2-}$, $SO_4^{2-}$, $Cl^{-}$, $HCO_3^{-}$, $CH_3COO^{-}$)**

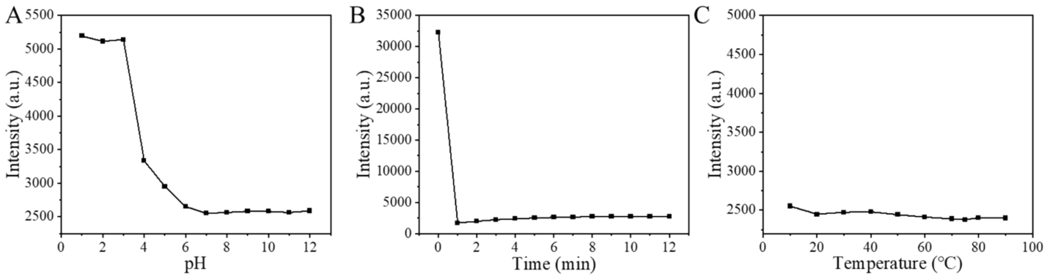


**Fig. S6 CDs at different (A) pH values; (B) Response time; (C) Temperature; The fluorescence intensity after adding $Fe^{3+}$ under certain conditions.**

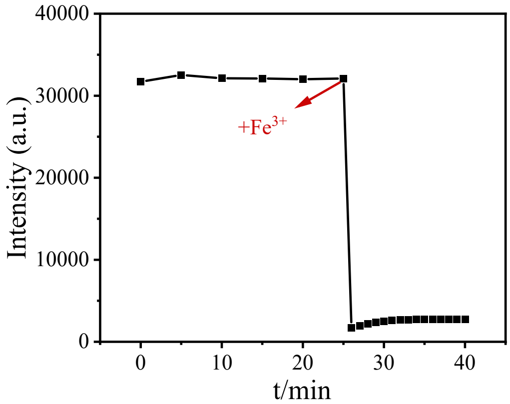


**Fig. S7 The fluorescence intensity of CDs before and after the addition of $Fe^{3+}$ over time.**

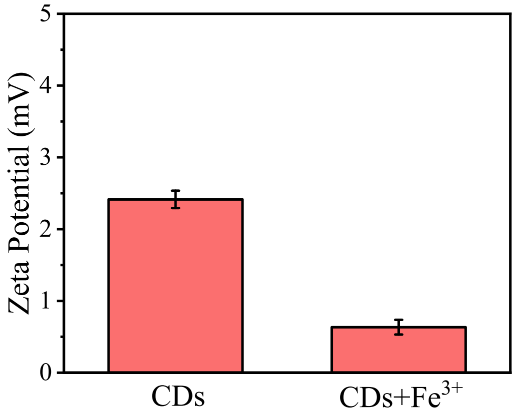


**Fig. S8 Zeta-Potential of CDs in the presence or absence of $Fe^{3+}$**

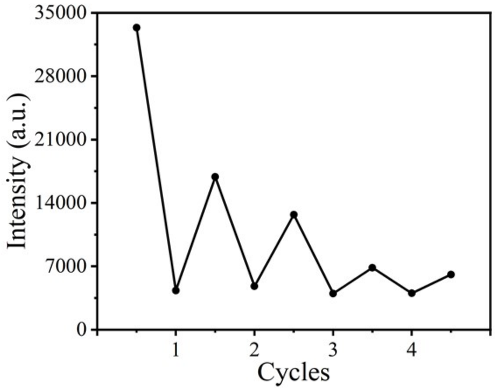


**Fig.S9 Repeated on-off switching of the fluorescence emission of CDs in $SiO_3^{2-}$ and $Fe^{3+}$ solution cycles.**

**Table S1. Comparison of CDs with existing coal-based carbon points**

| Carbon Precursor | Synthesis method | appliance | quantum yield | Ref. |
|---|---|---|---|---|
| coal-based humic acid | solvent heat | sensing of $H_2O_2$ | 7.6% | S1 |
| Coal-based humic acid | hydrothermal | | 14% | S2 |
| Low-rank coal | nitric acid oxidation | fluorescent inks | 9.11% | S3 |
| Lignite | ultrasound-assisted hydrogen peroxide | Detection of $Cr^{6+}$ | 1.37% | S4 |
| Anthracite and lignite | Sulfuric acid and nitric acid are mixed and oxidized | Anti-counterfeiting | 1.62% | S5 |
| raw coal | Mixed oxidation of $H_2O_2$ and $NH_3{\cdot}H_2O$ | Optoelectronic devices | 8.9% | S6 |
| coal washery rejects | | | 14.9% | |
| Coal | Mixed oxidation of $H_2O_2$ and HCOOH | Detection of $Fe^{3+}$ | 7.2% | S7 |
| Lignite | Oxidation of $H_2O_2$ | Detection of $Cu^{2+}$ | 0.81% | S8 |
| Coal pitch | Mixed oxidation of $H_2O_2$ and HCOOH | | 3.77% | S9 |
| Coal pitch | Hydrothermal in $H_2O_2$ and HCOOH solution | LED | 8.36% | S10 |
| Lignite | Chemical oxidation with $H_2O_2$ | Detection of $Fe^{3+}$ in soil | 23.49% | This work |

**Table S2. Comparison of the $Fe^{3+}$ detection limit between CDs and the existing CDs detection**

| Carbon Precursor | Synthesis method | Detection object | Detection limit | Ref. |
|---|---|---|---|---|
| citric acid | hydrothermal | $Fe^{3+}$ | 0.753 μM | S11 |
| waste egg tray paper pulp | hydrothermal | $Fe^{3+}$ | 1.418 μM | S12 |
| methionine | solvent heat | $Fe^{3+}$ | 7.12μM | S13 |
| citric acid | solvent heat | $Fe^{3+}$ | 4.5 μM | S14 |
| sodium citrate | hydrothermal | $Fe^{3+}$ | 1.41 μM | S15 |
| mushroom | hydrothermal | $Fe^{3+}$ | 16 μM | S16 |
| coffee grounds | solvent heat | $Fe^{3+}$ | 4.31 μM | S17 |
| Lignite | Chemical oxidation with $H_2O_2$ | $Fe^{3+}$ | 0.123 μM | This work |

**Table S3. Detection of $Fe^{3+}$ present in the original soil at different pH levels**

| Sample | pH value | Measured value of $Fe^{3+}$ (n=3) (μM) | Relative standard deviation (%) |
|---|---|---|---|
| Soil leachate | 2 | 0.79 | 1.52% |
| | 4 | 0 | -- |
| | 6 | 0 | -- |
| | 8 | 0 | -- |


[S1] He Z, Yuen M, Zhang C, et al. Room-temperature phosphorescence in coal-based humic acid-derived carbon dots[J]. Journal of Materials Chemistry C, 2024, 12(17): 6333-6340.

[S2] Song S, Wang Z, Pan C, et al. Achieving full-color emission in coal-based humic acid derived carbon dots through intradot aggregation[J]. Journal of Materials Chemistry C, 2022, 10(27): 10124-10131.

[S3] Jiang W, He H, Wang C, et al. Preparation of coal-based carbon quantum dots and their fluorescence properties[J]. Microchemical Journal, 2024, 207: 111818.

[S4] Xu S, Zhang J, Li M, et al. In situ synthesis of S-doped coal-based carbon quantum dots and its application to $Cr^{6+}$ detection[J]. Journal of Chemical Technology & Biotechnology, 2023, 98(10): 2532-2545.

[S5] Du M, Wang C, Liu X, et al. Morphological insights into uncompetitive fluorescence of coal-based carbon dots and strategies for improvement[J]. Carbon, 2024, 228: 119396.

[S6] Boruah A, Bora S, Thakur A, et al. Solid-state phosphors from coal-derived carbon quantum dots[J]. ACS omega, 2023, 8(28): 25410-25423.

[S7] Cheng Z, Wu X, Liu L, et al. A highly efficient, rapid, room temperature synthesis method for coal-based water-soluble fluorescent carbon dots and its use in $Fe^{3+}$ ion detection[J]. New Carbon Materials, 2023, 38(6): 1104-1115.

[S8] Shi C, Wei X Y, Liu F J, et al. Carbon Dots Derived from Facile Tailoring of Shaerhu Lignite as a Novel Fluorescence Sensor with High-Selectivity and Sensitivity for $Cu^{2+}$ Detection[J]. ChemistrySelect, 2020, 5(39): 12125-12130.

[S9] Meng X, Chang Q, Xue C, et al. Full-colour carbon dots: from energy-efficient synthesis to concentration-dependent photoluminescence properties[J]. Chemical communications, 2017, 53(21): 3074-3077.

[S10] Zheng Y, Ye S, Chang Q, et al. Tailoring the Optical Properties of Coal Pitch-Derived Carbon Dots by

Graphitization Controlling[J]. Energy & Fuels, 2024, 38(15): 14475-14482.

[S11] Li B, Wu F, Xie Z, et al. High acid-base tolerance and long storage time lanthanum cerium co-doped carbon quantum dots for $Fe^{3+}$ detection[J]. Spectrochimica Acta Part A: Molecular and Biomolecular Spectroscopy, 2025, 327: 125403.

[S12] Mahilary B, Patir K, Kandinya R, et al. Waste Egg Tray Paper Pulp Derived Carbon Dots for Detection of $Fe^{3+}$ Ions via Fluorescence On-Off Process[J]. Journal of Fluorescence, 2025: 1-10.

[S13] Yang C, Xu G, Hou C, et al. Ratiometric fluorescence nanoprobe based on nitrogen-doped carbon dots for $Cu^{2+}$ and $Fe^{3+}$ detection[J]. Scientific Reports, 2025, 15(1): 6261.

[S14] Jiang Y, Wang H, Nie T, et al. White-emissive boron and nitrogen co-doped carbon dots for detection of water in organic solvents and $Fe^{3+}$ ions[J]. Materials Today Communications, 2025, 44: 111992.

[S15] Guo S, Liang L, Guo Q, et al. Incorporating silicon-doped carbon dots into europium chelated silica microspheres for the ratiometric fluorescent and colorimetric detection of $Fe^{3+}$ ions[J]. Microchemical Journal, 2025: 115194.

[S16] Klongklaw K, Phiromkaew B, Kiatsuksri P, et al. Green one-step synthesis of mushroom-derived carbon dots as fluorescent sensors for $Fe^{3+}$ detection[J]. RSC advances, 2023, 13(44): 30869-30875.

[S17] Zhang B, Liu Z, Qian D, et al. Application of polyamide 56 nanofiber membrane loaded with coffee grounds carbon dots in $Fe^{3+}$ detection[J]. Spectrochimica Acta Part A: Molecular and Biomolecular Spectroscopy, 2025, 328: 125440.